J Mater Sci (2008) 43:4290–4296
DOI 10.1007/s10853-008-2626-x

Toughening effect of maleic anhydride grafted linear low density polyethylene on linear low density polyethylene

Le-Ping Huang · Xing-Ping Zhou · Wei Cui · Xiao-Lin Xie · Shen-Yi Tong

Received: 9 January 2008 / Accepted: 28 March 2008 / Published online: 9 April 2008

Abstract The blend of linear low density polyethylene (LLDPE) and maleic-anhydride grafted LLDPE with the grafting degree of 1.3% and the gel content of 27.0% (designated as LLDPE/MA-PE) was melt-compounded. Their thermal, rheological, and mechanical properties were studied. The crystallization temperature and crystallization rate of LLDPE/MA-PE blends increase due to the nucleation of MA-PE, their crystallinity is between those of LLDPE and MA-PE due to the balance between the nucleation of MA-PE and simultaneously produced more defects. The addition of MA-PE increases the apparent viscosity of blend melts, but the shear-sensitivity of blends provides them with melting processing. Interestingly, the lamellar crystallites induced by MA-PE decrease the tensile yielding strength of LLDPE/MA-PE blends. During the impact fracture, the formation of oriented crystalline lamellae parallel to the crack front and perpendicular to the crack flank, leads to the deformation and microstriations in LLDPE/MA-PE blends. Subsequently, toughness of LLDPE/MA-PE blends is improved.

L.-P. Huang · X.-P. Zhou · W. Cui · X.-L. Xie (✉)
Department of Chemistry and Chemical Engineering, Hubei Key Laboratory of Materials Chemistry and Service Failure, Huazhong University of Science and Technology, Wuhan 430074, China
e-mail: xlxie@mail.hust.edu.cn

X.-L. Xie
Center for Advanced Materials Technology, School of Aerospace, Mechanical and Mechatronic Engineering, J07, University of Sydney, Sydney, NSW 2006, Australia

S.-Y. Tong
Hubei Key Laboratory of Novel Reactor and Green Chemical Technology, Wuhan Institute of Technology, Wuhan 430073, China

Introduction

Linear low density polyethylene (LLDPE) is a class of polyethylenes with linear chains containing only short chain branching due to the insertion of α-olefin units during the copolymerization reaction of ethane with less than 10% of an α-olefin (e.g., hexene, butene, octene, etc.) [1]. LLDPE possesses superior processability and melt strength, good environmental stress, and cracking resistance, and has acquired a great commercial market in films, sheets, pipes, fibers, coatings, and molded articles, including containers and consumer goods. Most of the previous studies have used Ziegler–Natta LLDPE, which is known for its inter- and intra-molecular heterogeneity [2, 3], the development on metallocene technologies as a considerable advance improves its physical properties and enlarges its applications greatly [4]. On the other hand, functionalization of polyethylene via grafting with polar unsaturated monomers has attracted much attention due to the application in polymer blends and composites [5, 6]. Since there are side reactions including cross-linking, which leads to the high gel content during the grafting polymerization [7, 8], many efforts have been made to enhance the grafting degree and reduce the gel content. Gaylord additives (e.g., nitrogen-, phosphorous-, and sulfur-containing organic electron donors) could prevent cross-linking of polyethylene and homopolymerization of maleic anhydride (MAH) [9–12]. However, the above additives simultaneously decrease the grafting degree. On the other hand, the use of vinyl comonomers could

simultaneously increase the grafting degree and decrease the cross-linking of polyethylene [13–16]. Recently, the effects of polyethylene structure and molecular weight on grafting reaction were studied, and the functionalized polyethylene is widely used as compatibilizer in polymer blends and composites [17–20]. The blends of PE and other thermoplastics, such different type PE, polypropylene (PP), polystyrene (PS), polyamide 6 (PA-6), rubber, and other commodity polymers, has been reported [21], but the blend of polyethylene (PE) and its functionalized counterpart has not been systematically studied to our best knowledge. In this work, LLDPE was melt-compounded in a twin screw co-rotating extruder with MAH grafted LLDPE (designated as MA-PE) with the grafting degree of 1.3% and the gel content of 27.0%. The thermal, rheological, and mechanical properties of LLDPE/MA-PE blends were systematically studied, and the toughening effect of MA-PE on LLDPE was discussed.

Experimental

Sample preparation

LLDPE granules with melt flow index of 4.5 g/10 min (190 °C, 2.16 kg) were purchased from Qilu Petrochemical Co., Ltd (China) under a tradename of LLDPE 7149. MA-PE was synthesized by solid-state grafting technology with the above LLDPE, its grafting degree and gel content were determined to be 1.3% and 27.0%, respectively [22]. Briefly, LLDPE powders with diameter of about 0.9 mm and xylene as interfacial agent were mixed in a 10 L stainless steel jacket reaction vessel fitted with a helical scraper-type stainless steel agitator under nitrogen atmosphere. The stirring speed and reaction temperature were set as 60 rpm and 105 °C, respectively. MAH and BPO were divided into four equal parts by weight, and added into the reactor in 15-min intervals. The products were poured into hot water, washed alternately by xylene and ethanol for 3 cycles, dried in a vacuum at 80 °C for 24 h.

For preparation of LLDPE/MA-PE blends, the MA-PE weight fraction in LLDPE/MA-PE blends was 5, 7.5 and 10%, and the resultant blends were designated as LLDPE/MA-PE5, LLDPE/MA-PE7.5 and LLDPE/MA-PE10, respectively. Before melt blending, MA-PE powders were dried in an oven at 80 °C for 48 h. In the preparation of the nanocomposites, LLDPE granules and MA-PE powders were melt-compounded in GE-35 twin screw co-rotating extruder (L/D = 43, D = 35 mm; Nanjing Keya Rubber and Plastics Machinery Co., Ltd., China) at a screw speed of 50 rpm. The barrel temperature profile was set to 165, 170, 185, and 180 °C. The extrudates were pelletized at the die exit, dried, and injection molded to standard dumb-bell tensile bars and Izod notched impact specimen by XS-ZY-125 injection molding machine (Zhejiang Plastics Machinery Co. Ltd., China) whose injection barrel temperature profile was set to 165, 200, and 185 °C.

Characterization

Differential scanning calorimetry (DSC) analysis was conducted in a Perkin–Elmer DSC-7 instrument at a heating rate of 10 °C min^{-1} under dry nitrogen atmosphere. Prior to the DSC recording, all samples were heated to 180 °C and then kept at this temperature for 5 min to eliminate the influence of their previous thermal histories. They were finally quenched to an ambient temperature. For non-isothermal crystallization measurements, samples were heated to 180 °C at a rate of 10 °C/min, kept at 180 °C for 3 min, and then cooled to 30 °C at a rate of 10 °C/min.

Rheological properties were measured at 190 °C using a XLY-1 capillary rheometer (Jilin University Scientific Instrument Factory, China). The capillary die used had a length (L) to diameter (D) ratio of 40/1 and an entrance angle of 180°. The Rabinowitch correction was applied to all the experimental data, the Bagley correction was neglected since the L/D ratio was up to 40 [23].

Tensile tests were conducted on dumbbell shaped specimens with a WDW-2 tensile testing machine (Shenzhen Kaiqiang Testing Instruments Co. Ltd, China) at a crosshead rate of 20 mm/min according to GB/T 1040-92 standard. The notched Izod impact tests were conducted with a XJU-22 impact test machine (Chengde Testing Instruments Co. Ltd, China) at ambient temperature according to GB/T 1843–1996 standard. At least five samples of each composition were tested and mean values and standard deviations (SD) were calculated.

A Philips X'Pert Pro X-ray Diffractometer with Cu Kα radiation ($\lambda = 1.5406$ Å) at a generator voltage of 40 kV and a current of 40 mA was used. The samples were cut from the compression molded plates. All experiments were carried out in the 2θ range of 5–50° at ambient temperature with a scanning speed of 5°/min and step size of 0.02°.

Polarized optical microscope (POM) observation was performed by an Olympus BX 51 microscope equipped with a crossed polarizer and a hot stage. In order to observe the crystal morphology, the specimen was first melted at 200 °C and kept at this temperature for 3 min, and then was cooled down rapidly to the crystallization temperature (about 110 °C) and maintained for the time necessary for crystallization.

A commercial scanning electron microscope (SEM, JEOL JSM 5900LV) was employed to study the morphologies of fractured surface. The specimens were coated with a thin layer of gold prior to SEM examinations.

Results and discussion

Thermal properties

Figures 1 and 2 show the DSC heating and cooling curves of LLDPE, MA-PE, and LLDPE/MA-PE blends. Their peak melting temperature (T_{mp}), onset melting temperature (T_{m0}, determined as the temperature at the intercept of the tangents at the low temperature side of the endotherm and the baselin), crystallization temperature (T_c, determined as the temperature at the intercept of the tangents at the high temperature side of the exotherm and the baselin) and melting heat (ΔH_m) are given in Table 1.

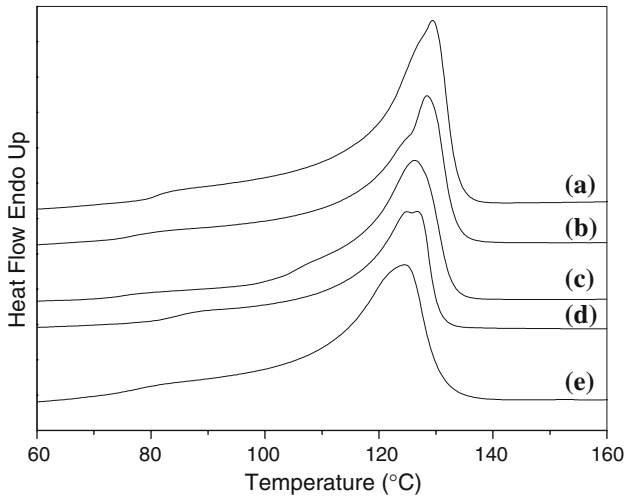

Fig. 1 DSC heating curves of LLDPE/MA-PE blends. (a) LLDPE; (b) LLDPE/MA-PE5; (c) LLDPE/MA-PE7.5; (d) LLDPE/MA-PE10; (e) MA-PE

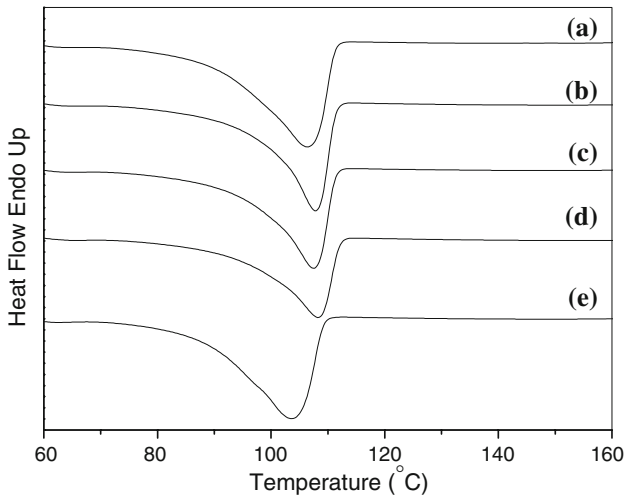

Fig. 2 DSC cooling curves of LLDPE/MA-PE blends. (a) LLDPE; (b) LLDPE/MA-PE5; (c) LLDPE/MA-PE7.5; (d) LLDPE/MA-PE10; (e) MA-PE

Table 1 Melting and crystallization parameters for LLDPE, MA-PE and LLDPE/MA-PE blends

Sample	T_{mp} (°C)	T_{mo} (°C)	T_c (°C)	ΔH_m (J/g)	ΔT (°C)	Xc (%)
LLDPE	129.6	117.3	106.6	94.4	23.0	33.8
MA-PE	125.6	117.0	103.1	87.7	22.5	31.4
LLDPE/MA-PE5	128.5	116.4	107.9	85.6	20.6	30.1
LLDPE/MA-PE7.5	126.7	115.4	107.7	90.2	19.0	32.3
LLDPE/MA-PE10	126.9	115.8	109.5	77.0	17.4	27.6

Generally, the degree of supercooling, ΔT, can be used to characterize the crystallization behavior of polymer melts. It is defined by the difference between the peak melting temperature and onset crystallization temperature. A decrease in ΔT generally indicates that the crystallization rate of polymer is accelerated. The degree of crystallinity (X_c) of LLDPE/MA-PE blend has been determined according to:

$$X_c = \frac{\Delta H_m}{\Delta H^*} \times 100\% \quad (1)$$

where ΔH_m is the melting heat of the LLDPE/MA-PE blend and ΔH^* is the melting heat of LDPE with 100% crystallinity. From literature [24], the value of ΔH^* for 100% crystalline LDPE is 279 J/g. The calculated X_c and ΔT values are also listed in Table 1.

From the above results, the melting temperatures (T_{m0} and T_{mp}) of LLDPE phase in LLDPE/MA-PE blends tend to decrease compared with those of pure LLDPE. Since MA-PE originates from LLDPE, and has the same main-chain backbone structure as LLDPE even though there exist some gels in MA-PE, LLDPE and MA-PE are compatible as reflected by the decrease in the melting temperatures of LLDPE/MA-PE blends based on Nishi and Wang' theory [25]. In addition, crystallization temperature (T_c) and crystallization rate (as reflected by the decrease in ΔT) of LLDPE/MA-PE blends increase due to the nucleation of MA-PE with gel content of 27%. However, X_c values of MA-PE and LLDPE/MA-PE blends are lower than that of LLDPE because the grafting of MAH onto LLDPE and cross-linking formation in MA-PE lead to more defects in crystals of MA-PE and LLDPE/MA-PE blends.

Rheological properties

The melt viscosity of polymer melts is an important parameter to evaluate their processing properties, the rheological behaviors of LLDPE and LLDPE/MA-PE blends were examined by a capillary rheometer at 190 °C, and the results are given in Fig. 3. Obviously, all of LLDPE and LLDPE/MA-PE blends exhibit non-Newtonian and shear thinning characteristics in the range of applied shear rates,

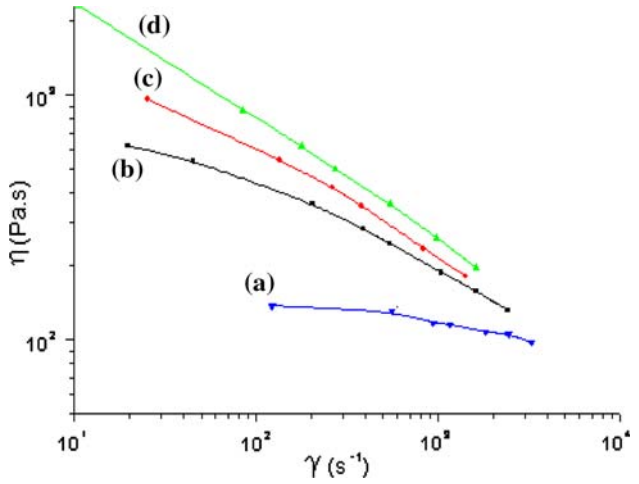

Fig 3 Rheological behavior of LLDPE/MA-PE blends. (a) LLDPE; (b) LLDPE/MA-PE5; (c) LLDPE/MA-PE7.5; (d) LLDPE/MA-PE10

the apparent viscosity of LLDPE/MA-PE blend is higher than that of LLDPE, and increases with the content of MA-PE with gel content of 27%. Interestingly, the shear-sensitivity of LLDPE/MA-PE blend is stronger than that of LLDPE, and the apparent viscosity values of LLDPE/MA-PE blends are closed to that of LLDPE at higher shear rate of about 2,000 s^{-1}, which indicates that the LLDPE/MA-PE blends can flow and be injection molded in the molten state.

Mechanical properties and fracture micromechanism of LLDPE/MA-PE blends

Figure 4 shows the effects of the MA-PE content on tensile and impact properties of LLDPE/MA-PE blends. It can be seen that the addition of MA-PE obviously increases the impact strength of LLDPE, but deceases the tensile yielding strength of LLDPE slightly. For example, the tensile yielding strength of LLDPE/MA-PE10 decreases to 14.0 MPa from 16.0 MPa of LLDPE, but its impact strength increases to 22.1 kJ/m^2 from 13.6 kJ/$m^2$of LLDPE, the increment is up to 61%. In order to gain a better understanding of the toughening mechanism, the crystalline structure and fractured morphology of LLDPE/MA-PE blends were characterized by wide-angle X-ray diffraction (WXRD), POM and SEM.

The WXRD patterns of LLDPE, MA-PE, and LLDPE/MA-PE10 blend are given in Fig. 5. LLDPE shows two strong diffraction peaks at 21.65 and 21.94°, which correspond to [1, 1, 0] and [2, 0, 0] diffractions of crystals with a monoclinic configuration, respectively. The diffraction patterns of MA-PE and LLDPE/MA-PE10 blend is the same as that of LLDPE. In order to study their crystal structure, peak-fit analyzing software was used to obtain a series of crystal parameters, such as interplanar space (d),

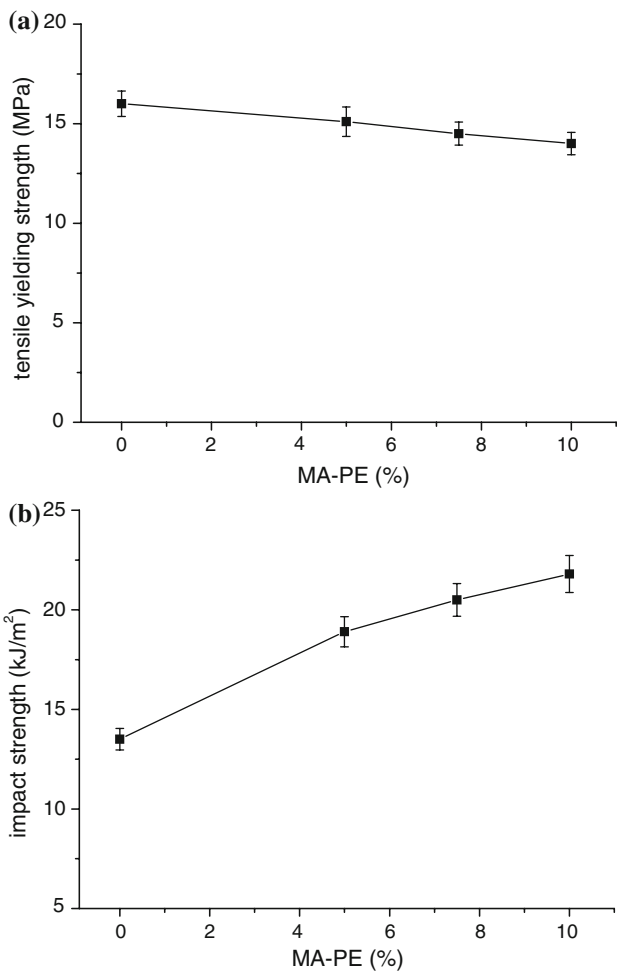

Fig. 4 Effects of the MA-PE content on mechanical properties of LLDPE/MA-PE blends. (**a**) Tensile yielding strength; (**b**) Impact strength

half-width (β), apparent crystal size (L_{hkl}) etc. The degree of crystallinity (X_c) are given by:

$$X_c = 1 - \frac{A_a}{A_c + A_a} \tag{2}$$

where A_a and A_c are the areas of the amorphous and the total crystal peaks, respectively.

The interplanar spacing (d) and apparent crystal size (L_{hkl}) values for the different peaks can be calculated by Bragg's law and Scherrer's formula [26], respectively.

$$d = \frac{\lambda}{2\sin\theta} \tag{3}$$

$$L_{hkl} = \frac{k' \times \lambda}{\beta_0 \times \cos\theta} \tag{4}$$

$$\beta_0 = \sqrt{\beta^2 - b_0^2} \tag{5}$$

where β_0 is the half-width of the reflection corrected for the instrumental broadening according to Eq. 5, β is the half-

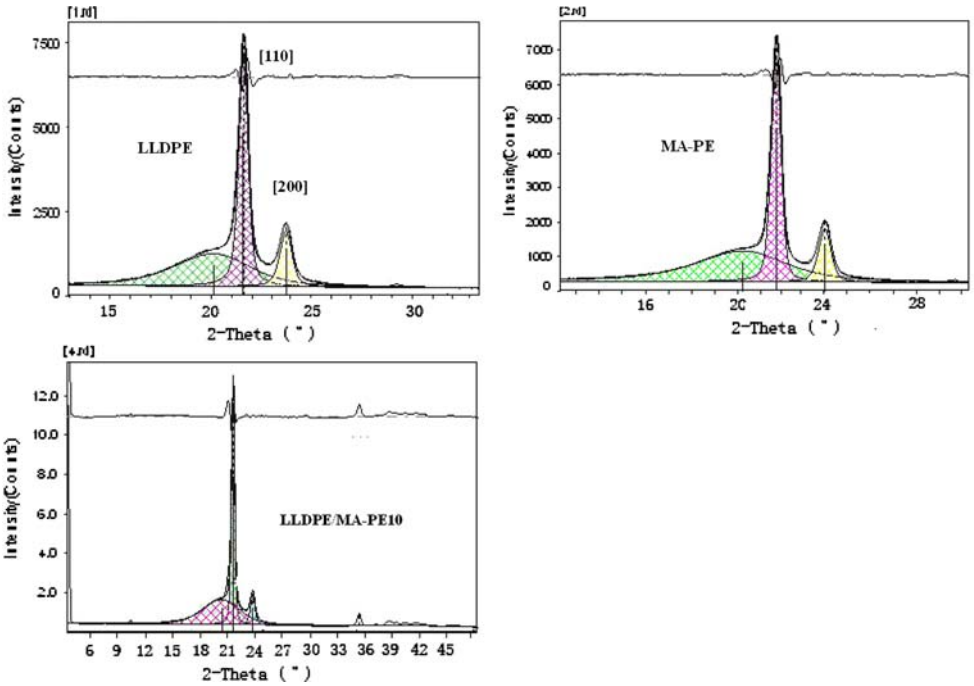

Fig. 5 WXRD patterns of LLDPE, MA-PE and LLDPE/MA-PE10 blend

width of various diffraction peaks, b_0 is the instrumental broadening factor (0.15°), λ is the wavelength of radiation used, and k' is the instrument constant (0.9).

Table 2 summarizes the crystal structural parameters determined based on WAXD curves. Compared with pure LLDPE, the interplanar spacing d values for various peaks of MA-PE show little change. It suggests that MAH is grafted onto LLDPE in the amorphous region during the solid-state grafting copolymerization. However, $L_{(110)}$ and $L_{(200)}$ of MA-PE tend to increase, and X_c of MA-PE decreases. The results further confirm that the grafting of MAH onto LLDPE and cross-linking lead to more defects in LLDPE crystals. Noticeably, $L_{(110)}$ and $L_{(200)}$ of LLDPE/MA-PE10 blend are larger than those of LLDPE and MA-PE, and X_c of LLDPE/MA-PE10 blend is between those LLDPE and MA-PE. The results suggest that MA-PE has a nucleation effect to LLDPE melting crystallization, incorporates more defects in LLDPE crystals simultaneously.

Table 2 Crystal structural parameters LLDPE, MA-PE and LLDPE/MA-PE10 blend

	Diffraction peak	2θ (°)	B_0 (°)	d (Å)	L_{hkl} (Å)	Xc (%)
LLDPE	110	21.65	0.53	4.1	146.8	53.9
	200	23.94	0.70	3.7	114.1	
MA-PE	110	21.72	0.48	4.1	159.5	48.7
	200	24.01	0.62	3.7	127.1	
LLDPE/MA-PE10	110	21.41	0.39	4.2	192.0	49.3
	200	23.68	0.60	3.8	132.8	

POM micrographs of LLDPE, MA-PE, and LLDPE/MA-PE10 blend are shown in Fig. 6. Obviously, pure LLDPE shows a typical banded spherulite structure with Maltese cross-pattern (see Fig. 6a), the maximum size of LLDPE spherulites is up to 80 μm. However, MA-PE forms the lamellar crystallites with the thickness of several micrometers and the length ranged from 5 to 50 μm (see Fig. 6b). Since the single lamellar crystals of polyethylene crystallized from solution have the thickness of 5–25 nm and the length of 1–50 μm [27, 28], the above lamellar crystallites is the aggregation of the single lamellar crystals because the gels in MA-PE induce LLDPE chains to fold and pack along the direction parallel to the interface between gel and LLDPE. It is similar with the results reported by Argon and his co-workers [29], i.e., the polyethylene lamellar crystallites preferentially grew 'edge-on,' in sheaf-like morphology, on the calcite or rubber interfaces with the crystallographic planes of the lamellae lying parallel to the interfaces. As discussed above, LLDPE and MA-PE are partially compatible, MA-PE uniformly dispersed in LLDPE matrix acts as a heterogeneous nucleating agent to induce LLDPE to form more lamellar crystallites (see Fig. 6c). The result are in accordance with the above WAXD analysis, are also confirmed by the lower tensile yielding strength of LLDPE/MA-PE blends than that of pure LLDPE.

Figure 7 is SEM micrographs of impact-fractured (at room temperature) and cryo-fractured surface near notch for LLDPE and LLDPE/MA-PE10 blend. Pure LLDPE shows a patch-like impact-fractured morphology (see Fig. 7a), but LLDPE/MA-PE10 blend exhibits the striation-type impact-fractured morphology (see Fig. 7b). The formation of these

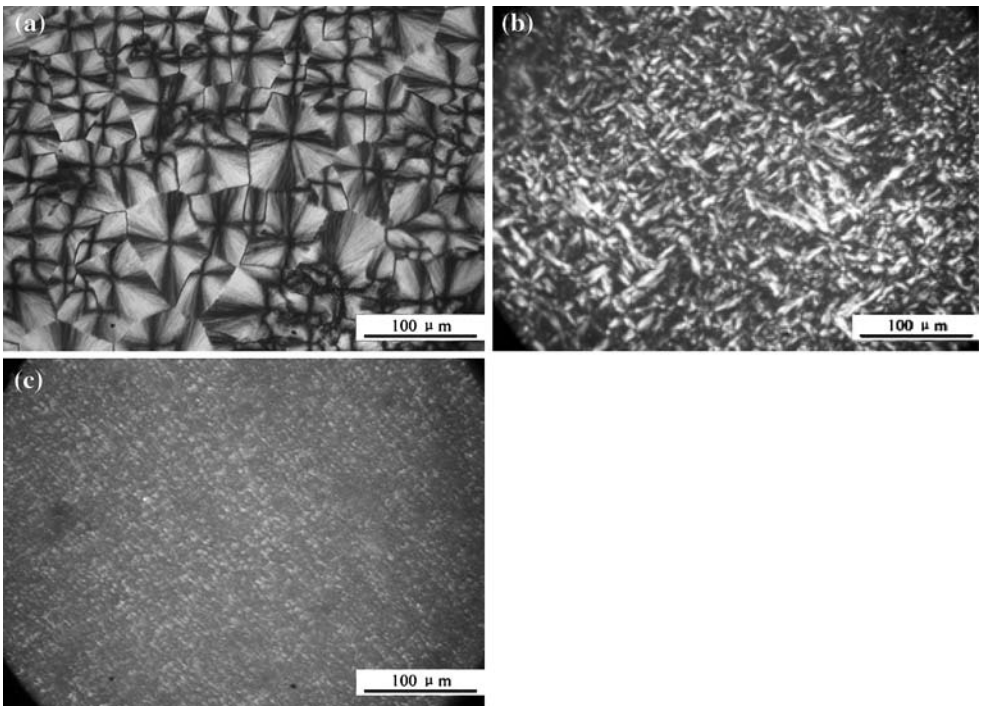

Fig. 6 POM micrographs of LLDPE (**a**), MA-PE (**b**) and LLDPE/MA-PE10 blend (**c**)

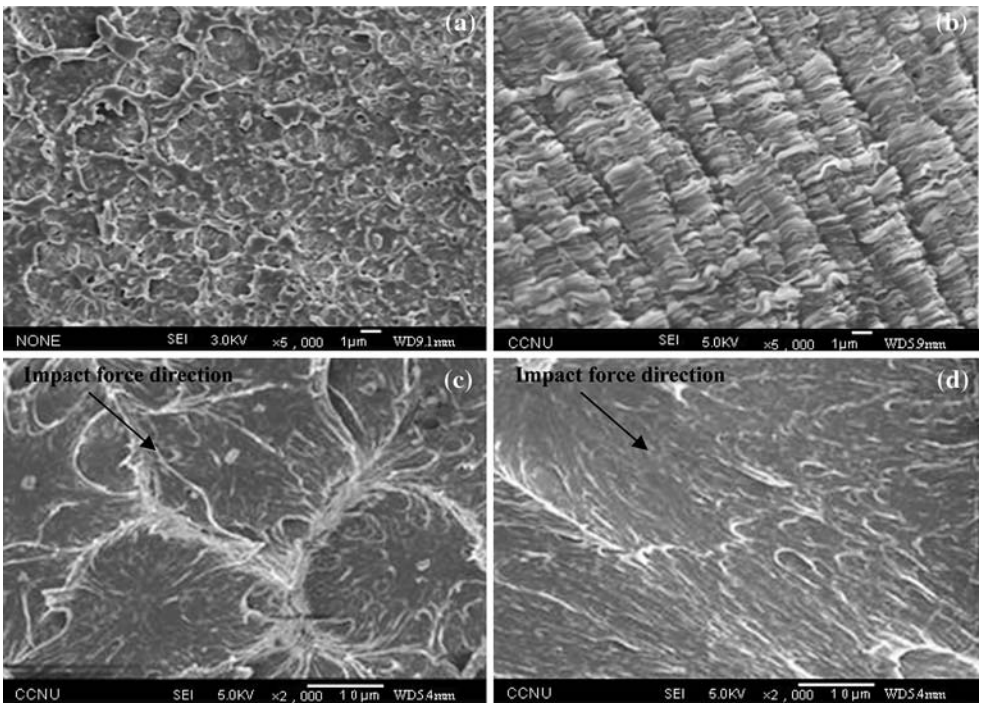

Fig. 7 SEM images of fracture surfaces of LLDPE and LLDPE/MA-PE10 blend. (**a**) LLEPE, fractured at room temperature; (**b**) LLDPE/MA-PE10 blend, fractured at room temperature; (**c**) LLDPE, cryo-fractured; (**d**) LLDPE/MA-PE10 blend, cryo-fractured

microstriations will absorb more impact energy and lead to toughening of the LLDPE/MA-PE blends. In order to further study the deformation of LLDPE and its blend in low temperature, LLDPE and LLDPE/MA-PE10 blend were cryo-fractured in liquid nitrogen. It can be seen that the deformation morphology of LLDPE is circle-like (see

Fig. 7c), but LLDPE/MA-PE10 blend deforms along the direction of impact force (see Fig. 7d). This is because crystals in LLDPE are spherulites, their deformations are isotropic. However, as discussed above, the crystals in LLDPE/MA-PE10 blend are lamellar. During the impact fracture, these crystalline lamellae are oriented parallel to the crack front and perpendicular to the crack flank, and the tensile yield strength of the LLDPE/MA-PE blend is lower than that of pure LLDPE. Thereby the LLDPE/MA-PE blend is easy to yield and deform under impact force. These factors lead to the formation of microstriations. Subsequently, these processes absorb more fracture energy, and toughen the LLDPE/MA-PE blend.

Conclusion

LLDPE/MA-PE blends were prepared by in a twin-screw co-rotating extruder. Due to the nucleation of MA-PE, the crystallization temperature and crystallization rate of LLDPE/MA-PE blends increase, but their degree of crystallinity is between those of LLDPE and MA-PE due to the balance between the nucleation of MA-PE and simultaneously produced more defects in LLDPE crystals. The addition of MA-PE increases the apparent viscosity of LLDPE/MA-PE blends, but the shear-sensitivity of LLDPE/MA-PE blends is stronger than that of LLDPE. At higher shear rate of about 2,000 s^{-1}, the apparent viscosity of LLDPE/MA-PE blends is close to that of LLDPE, which provides them with melting processability. In addition, the lamellar crystallites induced by MA-PE decrease the tensile yielding strength of LLDPE/MA-PE blends. During the impact fracture, these crystalline lamellae are oriented parallel to the crack front and perpendicular to the crack flank, which leads to the deformation of LLDPE/MA-PE blends and the formation of microstriations. These processes absorb more fracture energy, and subsequently toughen the LLDPE/MA-PE blends.

Acknowledgements The authors are grateful for the financial support of National Natural Science Foundation of China (50573026) and Program for New Century Excellent Talents in Universities of China (NCET-05–0640). As visiting professor of the Centre for Advanced Materials Technology (CAMT), the University of Sydney, XLX thanks Prof. Yiu-Wing Mai's academic guidance and help.

References

1. Kaminsky W (1992) In: Kricheldorf HR (ed) Handbook of polymer synthesis. Marcel Dekker, New York
2. Usami T, Gotoh Y, Takayama S (1986) Macromolecules 19:2722. doi:10.1021/ma00165a010
3. Freed KF, Dudowicz J, Freed KF, Dudowicz J (1996) Macromolecules 29:625. doi:10.1021/ma951062q
4. Bubeck RA (2002) Mater Sci Eng R 39:1. doi:10.1016/S0927-796X(02)00074-8
5. Moad G (1999) Prog Polym Sci 24:81. doi:10.1016/S0079-6700(98)00017-3
6. Russell KE (2002) Prog Polym Sci 27:1007. doi:10.1016/S0079-6700(02)00007-2
7. Porejko S, Gabara W, Blazejew T, Lecka M (1967) J Polym Sci Part A-1 Polym Chem 7:1647
8. Bray T, Damiris S, Grace A, Moad G, O'Shea M, Rizzardo E, Van Diepen G (1998) Macromol Symp 129:109
9. Gaylord NG, Mehta R (1988) J Polym Sci Part A Polym Chem 26:1189. doi:10.1002/pola.1988.080260419
10. Gaylord NG, Mehta R, Kumar V, Tazi M (1989) J Appl Polym Sci 38:359. doi:10.1002/app.1989.070380217
11. Gaylord NG, Mehta R, Mohan DR, Kumar V (1992) J Appl Polym Sci 44:1941. doi:10.1002/app.1992.070441109
12. Yang J, Yao Z, Shi D, Huang H, Wang Y, Yin J (2001) J Appl Polym Sci 79:535. doi:10.1002/1097-4628(20010118)79:3≤535::AID-APP170≥3.0.CO;2-L
13. Hegazy ESA, Taher NH, Ebaid AR, Rabie AG, Kamal H (1990) J Appl Polym Sci 39:1029. doi:10.1002/app.1990.070390502
14. Samay G, Nagy T, White JL (1995) J Appl Polym Sci 56:1423. doi:10.1002/app.1995.070561105
15. Cha J, White JL (2002) Intern Polym Process 17:115
16. Mahmoud GA (2007) J Appl Polym Sci 104:2769. doi:10.1002/app.25883
17. Machado AV, van Duin M, Covas JA (2000) J Polym Sci Part A Polym Chem 38:3919. doi:10.1002/1099-0518(20001101)38:21≤3919::AID-POLA90≥3.0.CO;2-L
18. Machado AV, Covas JA, van Duin M (2001) Polymer 42:3649. doi:10.1016/S0032-3861(00)00692-3
19. Razavi Aghjeh MK, Nazockdast H, Assempour H (2006) J Appl Polym Sci 99:141. doi:10.1002/app.21870
20. Sheshkali HRZ, Assempour H, Nazockdast H (2007) J Appl Polym Sci 105:1869. doi:10.1002/app.25391
21. Utracki LA (1998) Commercial polymer blends. Chapman & Hall, London
22. Tang JW, Tong SY (2007) Sci Technol Chem Ind 15(3):5 (in Chinese)
23. Brydson JA (1981) Flow properties of polymer melts, 2nd edn. George Godwin, London
24. Run MT, Gao JG, Li ZT (2005) Thermochim Acta 429:171. doi:10.1016/j.tca.2005.03.007
25. Olabisi O, Robeson LM, Shaw MT (1979) Polymer–polymer miscibility. Academic Press, New York
26. Alexander LE (1969) X-ray diffraction methods in polymer science. Wiley, New York
27. Till PH (1957) J Polym Sci 24:301. doi:10.1002/pol.1957.1202410616
28. Lin L, Argon AS (1994) J Mater Sci 29:294. doi:10.1007/BF01162485
29. Bartczak Z, Argon AS, Cohen RE, Kowalewski T (1999) Polymer 40:2367. doi:10.1016/S0032-3861(98)00443-1